RESEARCH ARTICLE

Polyoxotungstate/Oxy-Graphene Nanocomposite Multilayer Films For Electrocatalytic Hydrogen Evolution

Yasemin Torlak[1]* ✉ iD

[1] Pamukkale University, 20700, Denizli, Turkey.

Abstract: In this study, nanocomposites were formed together with Keggin-type $K_{7-x}Na_xPW_{11}O_{39} \cdot 14H_2O$ polyoxotungstates (POTs) clusters and oxygenated-graphene (Oxy-G). It was produced as a multilayer via layer-by-layer self-assembly method using protonated poly (ethylenimine) (PEI). The produced $(PEI/POTs/Oxy-G)_n$ multilayer films were controlled by XRD, cyclic voltammetry, and UV-Visible spectrophotometry. $(PEI/POTs/Oxy-G)_n$ multilayers are modified on a glassy carbon electrode. The hydrogen evolution reaction takes place by taking advantage of the electrocatalytic activity of this nanocomposite. They have been shown to exhibit a potentially good electrocatalytic activity at -0.4 V. A notable electrocatalytic hydrogen evolution reaction could be identified on the $(PEI/POTs/Oxy-G)_n$ multilayer. We demonstrate that expanded the application of POTs/G nanocomposites to the electrocatalysis of oxygen reduction reaction and hydrogen evolution reaction. This excellent approach will offer new insights into different electrode structure and the development of novel electroactive catalysts.

INTRODUCTION

Recently, global energy crisis externalized in the consuming of fossil fuels and the enlarging menace of environmental contamination, has induced a unique endeavor for the improve of novel renewable conversion technologies and energy storage, operating maintainable different chemical methods (1). Hydrogen can be an alternative for renewable and environmentally friendly fossil fuels of the next generation (1–2). Hydrogen production by the electrocatalytic reduction method provides a simple and effective solution for future energy demands. Graphene has recently been the focus of research because of unique surface area, electrical conductivity, and mechanical strength (1). The properties possessed of this advantage for graphene is the most remarkable materials for methods of immobilizing it into functional molecules (2). At the same time, these functional molecules can be adsorbed onto the graphene surface. Currently, metals (3), polymers (4), noble metals (5),

semiconductors (6), inorganic nanoparticles (7) enzymes (8) have been used to build graphene containing hybrid composites, and generally used in different fields such as supercapacitors and biosensors (9), photocatalysts or electrocatalysts (10) and lithium-ion batteries (11). Polyoxotungstates (POTs) are another vast class of well-defined, early transition metal-oxo clusters with different properties, sizes, nuclearities, and shapes. They are widely used as an electrocatalyst in the field of photocatalysis and electrocatalysis (11-13).

POTs/graphene (POTs/G) nanocomposites have significant improvements in different applications with the catalytic properties of POTs. Essentially, such an idea firstly derived from graphene oxide/POMs (Polyoxometalates) (14-15). The first studies on POTs/G nanocomposites and the experimental results were evaluated by Zhou in 2010 (16-20). First, phosphomolybdic acid was synthesized and then graphene composites were formed by hydrazine hydrate with POM

compound. Guo formed the graphene-modified electrode in a solution prepared with the Ru-POT compound dissolved in water and formed the Ru-POT / G composite structure for use as an electrocatalyst (18). Both Li (19) and Wang (20) studied different electrochemical methods to produce POT/G composites with electron-rich POTs. These studies with regard to the properties of POTs/G composites investigated as the microelectrodes used for generally in areas like photodetector devices, sensors to detect H_2O_2, catalysts for water oxidation, (18) and methanol oxidation (21). For oxygen reduction reaction (ORR) and hydrogen evolution reaction (HER) (22), there is not much research on the development of POTs/G electrocatalysts. A powerful and non-expensive electrocatalyst for ORR is important component for speeding the extensive trading of proton exchange membrane fuel cells.

In this study, synthesis of POT material acting as an electrocatalyst was made and then composite material was formed with graphene. Nanocomposite based on the Keggin-type POT clusters and oxidized graphite flakes was formed and we showed that these are structures exhibiting electrocatalytic activity for HER. In addition to the formation of POT-Oxy-G nanocomposite, there is not much work on electrocatalytic application for HER. POT clusters were immobilized via a one-step electroreduction synthesis on reduced oxidized graphite flakes. We contribute the high performance of our POT/Oxy-G hybrid catalyst in the HER to strong chemical and electronic coupling between the Oxy-G and POT. Chemical coupling/interactions afforded the selective growth of extremely dispersed POT nanoparticles on Oxy-G free of aggregation. The small size and high dispersion of Oxy-G and POT afforded an plenty of penetrable edges that could operate as active catalytic sites for the HER. Electrical coupling to the underlying Oxy-G in an interconnected conducting network afforded rapid electron transport from the less-conducting POT nanoparticles to the electrodes. Thus, the approach of materials composite on graphene has led to an advanced POTs electrocatalyst with highly competitive performance relative to various HER electrocatalytic materials.

MATERIALS AND METHODS

Materials and Instrumentation
Quartz slides, graphite flakes and silicon wafer and all chemicals were purchased from Aldrich. All the chemicals were used directly without any purification.

Instruments
UV-Vis spectral calculations were evaluated on a Hitachi-U4100 UV-Vis-NIR model spectrophotometer and IR spectra with a Nicolet 6700 FTIR model spectrometer. X-ray diffraction (XRD) patterns results were performed under a Bruker D8 Advance X-ray difractometer using Cu

Kα radiation λ = 1.5406 Å. AFM images were recorded on an (NT-MDT,Ntegra Solaris) model in tapping mode. The electrochemical behavior of nanocomposite was investigated by cyclic voltammetry with CH instruments 660B electrochemical workstation model in acetonitrile at a glassy carbon electrode, by using tetrabutylammonium tetrafluoroborate (NBu_4BF_4) as the supporting electrolyte. Platinum wire was used as the counter electrode and Ag/AgCl (KCl saturated) as reference electrode and a glassy carbon electrode as working electrode. The electrochemical behavior of nanocomposite was investigated by cyclic voltammetry with CH instruments 660B electrochemical workstation model in acetonitrile at a glassy carbon electrode, by using NBu_4BF_4 as the supporting electrolyte. All electrochemical measurements throughout the experiment were carried out at room temperature under nitrogen atmosphere. All cyclic voltammetric and amperometric measurements were carried out by this system.

Preparation of $K_{7-x}Na_xPW_{11}O_{39}\cdot14H_2O$ (POTs)
$Na_2WO_4.2H_2O$ (181.5 g, 0.550 mol) is dissolved in 300 mL of water and 50 mL of 1M H_3PO_4 is added followed by 88 mL of CH_3COOH. The solution is refluxed for 1 hour then potassium chloride (60 g, 0.805 mol) is added. The resulting white residue was filtered and washed with water and then dried to give POT (Yield: 104.4 g, 58%) (24).

Preparation of Oxygenated Graphene (Oxy-G)
GO was synthesized following Hummer's method. H_2SO_4, $NaNO_3$, and $KMnO_4$ were mixed together and reacted with natural graphite powder. Upon completion of the reaction, H_2O_2 was added onto this mixture. The resulting Oxy-G was separated by centrifugation and washed three times with 1 M hydrochloric acid solution, then washed with distilled water ten times to rinse. The product was dried in vacuum to afford brown sheets. Oxy-G dispersion was prepared by ultrasonically dissolving a required amount of Oxy-G solid into deionized water (10-11).

Preparation of POTs/Oxy-Graphene
Oxy-G dispersion was prepared for use in the reduction process. The synthesized POT compound and Oxy-G dispersion were mixed together to provide a homogeneous mixture. Then, pH =1.0 H_2SO_4 was added. In a three-electrode conventional glass cell, POT and Oxy-G mixture by means of cyclic voltammetry were measured in the acetonitrile solvent in the electrolyte solution. The POTs completely reduced on working electrode. Thanks to the multiple electrons found in the structure of the POT compound with the help of electrochemical and chemical processes, its redox state changes quickly. After completion of the electrochemical reduction process, POT/Oxy-G adsorbs on the glassy carbon electrode. This nanocomposite

formed was subjected to a vacuum oven at 80°C for 24 h.

Multilayer Assembly
Substrates were fabricated multilayer films via studies in the literature (23). The fabrication of POT/Oxy-G nanocomposite is shown schematically in Figure 1. The surface was immersed in PEI (polyethylenimine) solution (2 mg/mL, pH:7) solution for 20 minutes to load the surface with positive charges. The distillate was then washed with water and dried with nitrogen gas. Substrates coated with PEI were after immersed in a solution of POT (1 mg/mL) and Oxy-G (0.5 mg/mL) in pH 6.2 for 20 minutes.
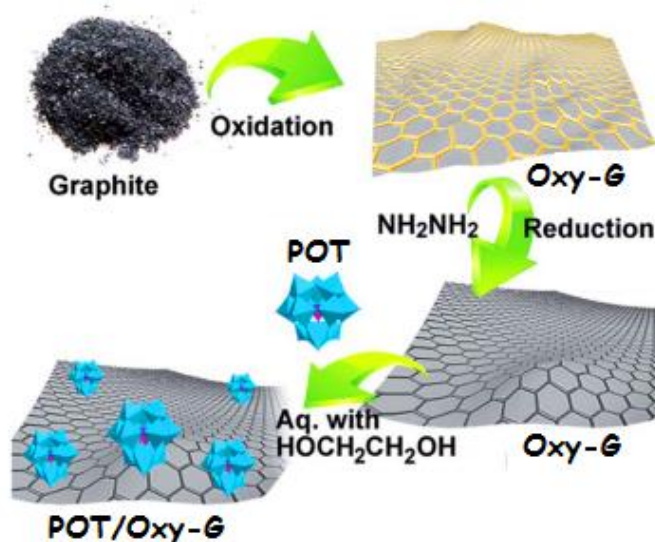
Figure 1. Schematic representation of the fabrication of POT/Oxy-G nanocomposite.

A nanocomposite was formed by the electrostatic interaction between the positively charged PEI and negatively charged POT/Oxy-G layer. And, then the distillate was then washed with water and dried with nitrogen gas. This procedure is repeated when multiple layers are formed. This is called a multilayer (PEI/POT/Oxy-G)$_n$ (n:number of multilayers)

RESULTS AND DISCUSSION

Growth of Multilayers
With the help of cyclic voltammetric (CV) methods and for UV-Visible spectroscopy, the growth of PEI/POT/Oxy-G)$_n$ multilayer film was controlled. On a quartz slide as shown in Figure 3 was evaluated the UV−Visible spectra of (PEI/POT/Oxy-G)$_n$ multilayers with a number ranging from one to eleven deposited. As shown in the inset of Figure 3, when UV-Visible absorption spectrum are evaluated, electrons are transferred from the oxygen atom to the tungsten atom and the values 215 and 270 nm are calculated.

These spectra show the presence of multiple layers and show that the POT compound is well incorporated into the Oxy-G structure. Characteristic bands and comparisons with each other can be seen in the UV-Vis spectral results. POT and Oxy-G structures overlap with each other, which is shown in Figure 3, but it is not clear based on this metamorphism that multiple layers are formed. Due to these reasons (PEI/POT/Oxy-G), other methods are used to show that multiple layers are formed. Figure 2 demonstrated that the cyclic voltammograms of the multilayer structures (PEI/POT/Oxy-G) with one to ten layer counts were taken on a glassy carbon electrode surface with 5×10^{-3} mol/L of TBABF in acetonitrile solutions.

The electrochemical window was set between 0 and -1.5 V outside which, towards more negative values. In Figure 2a, compared to the voltammograms, there were three redox peaks in the cyclic voltommogram of the POT compound, as shown in Figure 2b, but this peak was turned into five peaks when the composite was formed. They exhibit several reversible redox waves and this property can be exploited for construction of electrocatalytic hydrogen evolution.
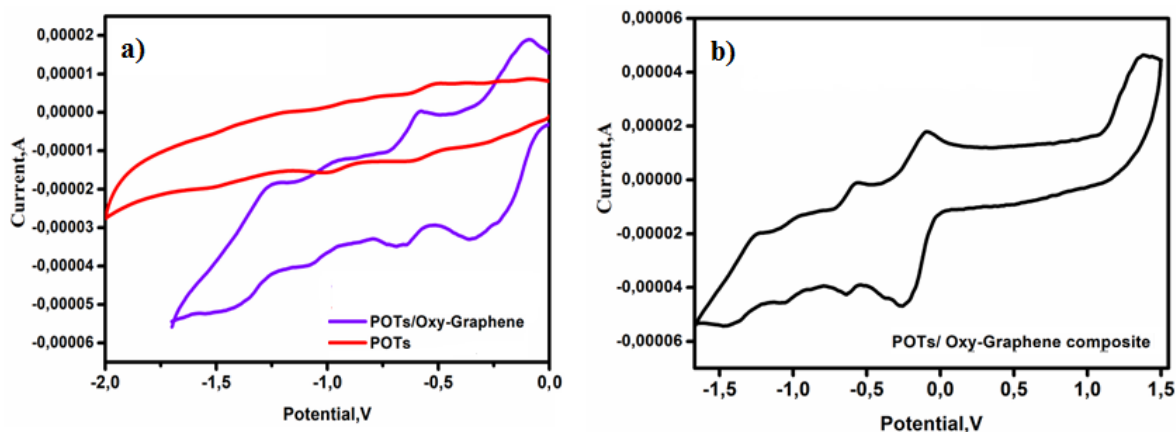
Figure 2. Cyclic voltammograms of a) POTs and POTs/Oxy-G b) (PEI/POT/Oxy-G)$_{10}$ multilayers deposited on GCE in 5 × 10^{-3} mol/L acetonitrile solution at 100 mV/s scan rates.

Due to the presence of many electrons in the POT structure and the presence of reversible redox peaks (−0.215, −0.317, −0.392, −0.446, and −0.598 V) potential changes are clearly visible in the nanocomposite structure. More than these redox peaks are because of the fact that the POT compound has undergone two successive electron transfer processes and the transition metal nature of this compound. As the number of layers increased, the current in the redox peaks increased. Although the Oxy-G structure is not very good in terms of electrical conductivity, there is no negative change in the electrochemical property of the POT compound while forming a multiple layer. And there is no change in the redox peaks in the cyclic voltammogram during

magnification of the (PEI/POT/Oxy-GO)$_n$ multilayers. At the same time the (PEI/POT/Oxy-GO)$_n$ multilayers showed a smooth growth without any peak potential change in the CV.

Spectral Characterization of (PEI/POT/Oxy-G)$_n$ Multilayers

(PEI/POT/Oxy-G)$_{10}$ multilayer was observed to change color when exposed to UV light. As shown in Figure 3, this multilayer and only the UV-Visible absorption spectra of the POT compound are comparable. This can be interpreted as an increase of the absorbance of the multilayers from 250 to 700 nm compared to the POT compound.
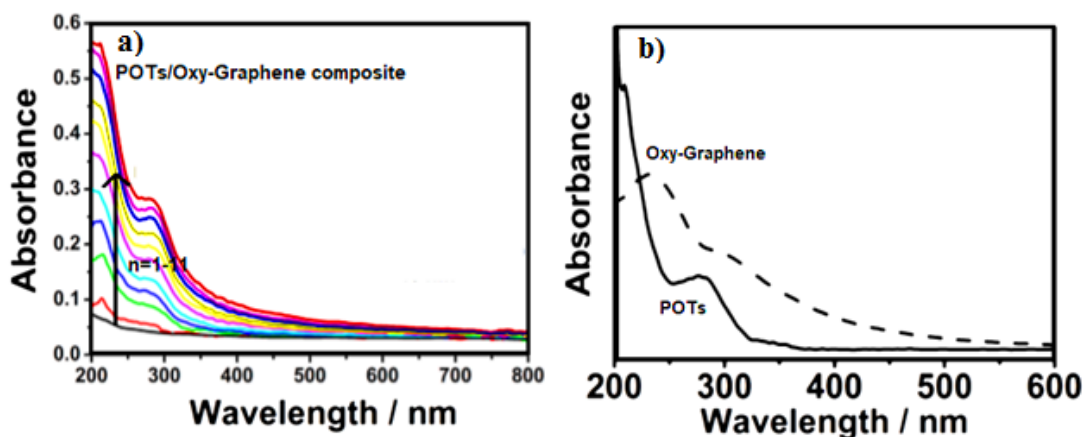
Figure 3. Absorption spectra of (PEI/POT/Oxy-G)$_{10}$ multilayers before a) and after b) exposure to UV light.

Figure 4 shows the XRD patterns of POT and POT/Oxy-G. As shown in Figure 4b, the sharp peak centered at 2θ = 28.5° corresponds to the (002) interplanar spacing of 0.35 nm in Oxy-G. After the composite is formed, diffraction angle of

POT appears to be shifting to higher. The presence of oxygen-bearing groups such as epoxides, hydroxyls, and carboxyls increased the basal spacing of Oxy-G after the process.
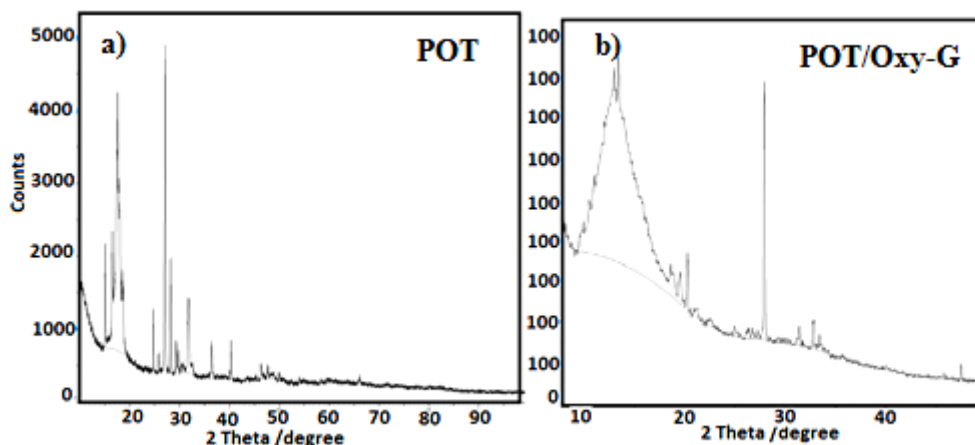
Figure 4. X-ray diffraction patterns of a) POT and b) POT/Oxy-G.

AFM (Atomic Force Microscopy) images of (PEI/POT/Oxy-G)$_3$ multilayers coated on silicon wafer are obtained for the morphological characteristic. In Figure 5a, it is clearly seen that some of the lamellar films were dimly visible with the appearance of aggregated nanoparticles underneath. As shown in Figure 5b, granular texture showed the morphology of the multilayers was composed of POTs and Oxy-G. Two types of negatively charged species, POT and Oxy-G were demonstrated to be distributed in the multilayers.
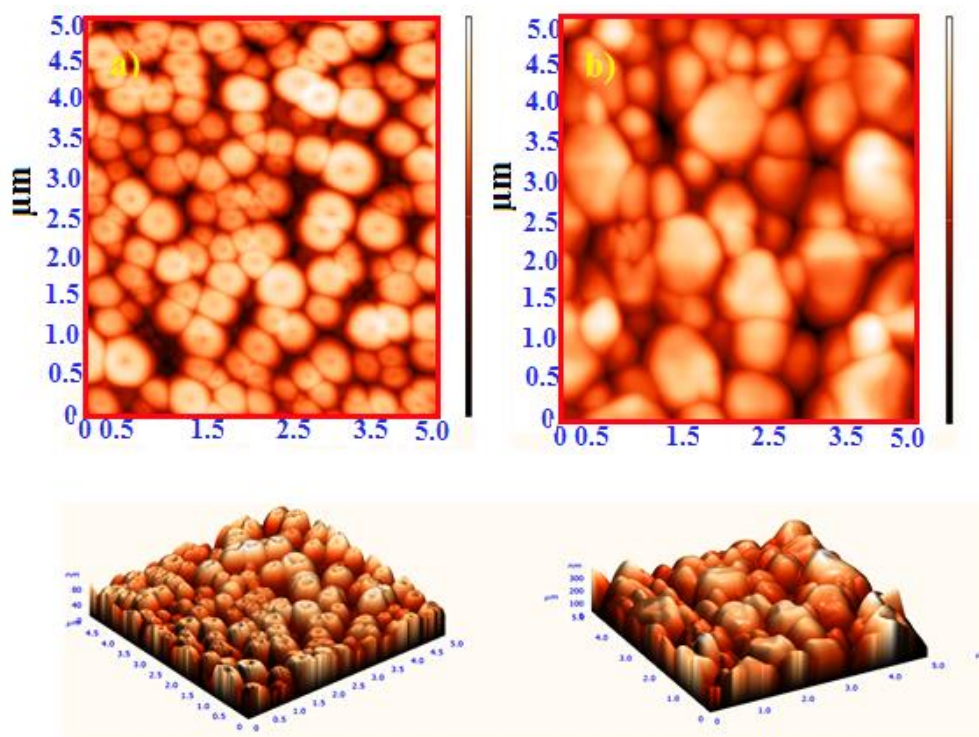
Figure 5. AFM images of a) POT and b) (POT/Oxy-G)$_3$ multilayers on silicon wafer at different scales.

It is foreseen that these changes will be due to the conjugated aromatic structure when electrons are transferred to the Oxy-G structure (17).

Figure 6a-b displays scanning electron microscopy (SEM) images of POT and POT/Oxy-G composites. Surface analysis with SEM is essential concerning the interaction of Oxy-G with POT surface and the observation of the morphological changes occurring on the surface of POT. As for this purpose, SEM images were recorded to verify the interaction of the synthesized POT with Oxy-G surface (Figure 6b). The Oxy-G exhibits porous architecture composed of ultrathin nanosheets conformed to electrically conductive framework beneficial for electron transfer and ion transport while maintaining electrical conductivity with substantial accessible specific surface area for ion sorption. As shown in Fig.6b., POTs appears to be distributed relatively uniformly over or within the Oxy-G nanosheets as aggregated molecular clusters with average size

graphene sheet edges and regions where the sheets are either folded or crumpled.

Electrocatalytic Behavior of POTs/Oxy-G Multilayers toward Hydrogen Evolution Reaction

The electrocatalytic activity of POTs/Oxy-G multilayers immobilized on glassy carbon electrode (GCE) toward HER was investigated. As shown in Figure 7, HER did not occur on the bare GCE before the potential of -0.8 V in 5×10^{-2} mol/L H_2SO_4 aqueous solution. When (POTs/Oxy-G)$_{10}$ multilayers were immobilized on GCE, the (POTs/Oxy-G)$_{10}$ multilayers exhibited good electrocatalytic activity for HER with a rapid increase in the cathodic peak current. This result indicates that the POTs/Oxy-G multilayer played a crucial role in electrocatalyzing HER.
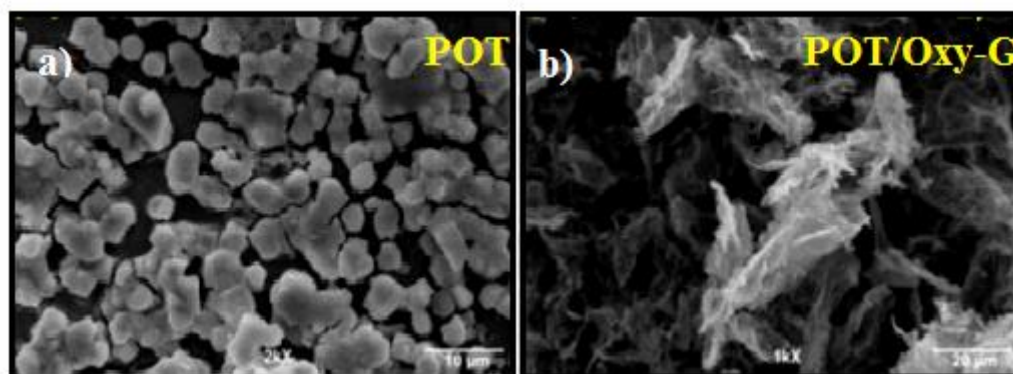
Figure 6. SEM images of a) POT (10 μm) and b) (POT/Oxy-G)$_3$(20 μm) multilayers on silicon wafer at different scales.
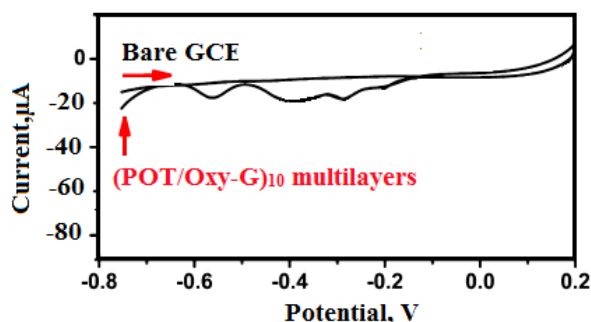
Figure 7. Linear sweep voltammograms of bare GCE and (POTs/Oxy-G)$_{10}$ multilayers in a 5×10^{-2} mol/L H_2SO_4 at a scan rate of 50 mV/s.

CONCLUSIONS

POTs/Oxy-G multilayer nanocomposite was formed with Keggin type polyoxotungstates (POT) and oxygenated-graphene (Oxy-G) together by postphotoreduction method and LbL self-assembly technique. The POT compound and Oxy-G together were deposited on different substrates utilizing the synergistic and electrostatic interaction between these two compounds. These two compounds are covered every step of the way and this number may vary depending on the desired operation. The transfer of electrons between PEI and Oxy-G can be successfully achieved by the successful transfer of charge transfer between POT and PEI. The photoreduction process is carried out under UV light and the POT compound acts as both a photocatalyst and an electron-transfer mediator to reduce the Oxy-G structure and provides a structural advantage in the formation of multiple layers. The (PEI/POT/Oxy-G)$_n$ multilayer formation provides a different structure for use in

electrocatalytic field. The electrocatalytic activity for the ORR application is the desired level, since the POT compound is unique in electrochemical aspects. In addition, these multilayers are clearly audible due to the presence of the Oxy-G signal. A synthetic approach in this way offers the opportunity as an alternative method of applying POTs/Oxy-G multilayer nanocomposites ORR and HER electrocatalysis. With the advantage of electronic interaction between POT and Oxy-G in addition to the accessible and reversible redox behavior of POTs, they could have different applications as a design of functional molecular materials or future generation of hybrid molecular devices.

REFERENCES

1. Geim AK, Novoselov KS. The rise of graphene. Nature Materials.2007 Mar; 6(3): 183−191.

2. Xie GC; Zhang K, Guo BD, Liu Q, Fang L, Gong JR. Graphene-based materials for hydrogen

generation from light-driven water splitting. Adv. Mater. 2013 Jul; 25(1): 3820−3839.

3. Kim YK, Han SW, Min DH. Graphene oxide sheath on Ag nanoparticle/Graphene hybrid films as an antioxidative coating and enhancer of surface-enhanced Raman scattering. ACS Appl. Mater. Interfaces. 2012 Sep; 4: 6545−6551.

4. Seger B, Kamat PV. Electrocatalytically active Graphene-Platinum nanocomposites. Role of 2-D carbon support in pem fuel cells. J. Phys. Chem. C. 2009; 113: 7990−7995.

5. Zhang K, Zhang LL, Zhao XS, Wu J. Graphene/Polyaniline nanofiber composites as supercapacitor electrodes. Chem. Mater. 2010; 22: 1392−1401.

6. Williams G, Seger B, Kamat PV. TiO_2-Graphene nanocomposites. UV-Assisted photocatalytic reduction of Graphene oxide. ACS Nano. 2008; 2: 1487−1491.

7. Wang QH, Jiao LF, Du HM, Wang YJ, Yuan HT. Fe_3O_4 nanoparticles grown on Graphene as advanced electrode materials for supercapacitors. J. Power Sources. 2014; 245: 101−106.

8. Zeng G, Xing Y, Gao J, Wang Z, Zhang X. Unconventional Layer-by-Layer assembly of Graphene multilayer films for enzyme-based glucose and maltose biosensing. Langmuir. 2010; 26: 15022−15026.

9. Liu R, Li S, Yu X, Zhang G, Zhang S, Yao J, Keita B, Nadjo L, Zhi L. Facile synthesis of Au-nanoparticle/Polyoxometalate/Graphene tricomponent nanohybrids: An enzyme-free electrochemical biosensor for hydrogen peroxide. Small. 2012 May;8(9):1398-406.

10. Zhang QL, Xu TQ, Wei J, Chen JR, Wang AJ, Feng JJ. Facile synthesis of uniform Pt nanoparticles on polydopamine-reduced Graphene oxide and their electrochemical sensing. Electrochim. Acta. 2013; 112: 127−132.

11. Xu CH, Xu BH, Gu Y, Xiong ZG, Sun J, Zhao XS. Graphene-based electrodes for electrochemical energy storage. Energy Environ. Sci. 2013; 6: 1388−1414.

12. Stracke JJ, Finke RG. Electrocatalytic water oxidation beginning with the Cobalt Polyoxometalate $Co_4(H_2O)_2(PW_9O_{34})_21O^-$:Identification of heterogeneous CoO_x as the dominant catalyst. J. Am. Chem. Soc. 2011; 133: 14872−14875.

13. Coquelard CC, Sébastien Sorgues S, Ruhlmann L. Photocatalysis with polyoxometalates associated to porphyrins under visible light: An application of charge transfer in electrostatic complexes. J. Phys. Chem. A. 2010; 114: 6394−6400.

14. Kovtyukhova NI, Ollivier PJ, Martin BR, Mallouk TE, Chizhik SA, Buzaneva EV, Gorchinskiy AD. Layer-by-Layer assembly of ultrathin composite films from micron-sized graphite Oxide sheets and polycations. Chem. Mater. 1999; 11: 771−778.

15. Petit C, Bandosz TJ. Graphite Oxide/Polyoxometalate nanocomposites as adsorbents of ammonia. J. Phys. Chem. C. 2009; 113: 3800−3809.

16. Zhou D, Han BH. Graphene-based nanoporous materials assembled by mediation of polyoxometalate nanoparticles. Adv. Funct. Mater. 2010; 20: 2717−2722.

17. Li HL, Pang SP, Wu S, Feng XL, Müllen K, Bubeck C. Layer-by-Layer assembly and UV photoreduction of Graphene-Polyoxometalate composite films for electronics. J. Am. Chem. Soc. 2011; 133: 9423−9429.

18. Guo SX, Liu YP, Lee CY, Bond AM, Zhang J, Geletii YV, Hill CL. Graphene-supported $\{Ru_4O_4(OH)_2(H_2O)_4\}^-$(Gamma-$SiW_{10}O_{36})_{21}^{0-}$ for highly efficient electrocatalytic water oxidation. Energy Environ. Sci. 2013; 6: 2654−2663.

19. Li SW, Liu RJ, Ngo Biboum R, Lepoittevin B, Zhang G, Dolbecq A, Mialane P, Keita B. First Examples of Hybrids Based on Graphene and a Ring-Shaped Macrocyclic Polyoxometalate: Synthesis, Characterization, and Properties. Eur. J. Inorg. Chem. 2013: 1882−1889.

20. Wang S, Li HL, Li S, Liu F, Wu DQ, Feng XL, Wu LX. Electrochemical-reduction-assisted assembly of a Polyoxometalate/Graphene nanocomposite and its enhanced lithium-storage performance. Chem. Eur. J. 2013; 19: 10895−10902.

21. Liu RJ, Li SW, Yu XL, Zhang GJ, Zhang SJ, Yao JN, Zhi LJA. General green strategy for fabricating metal nanoparticles/Polyoxometalate/Graphene tri-component nanohybrids: enhanced electrocatalytic properties. J. Mater. Chem. 2012; 22: 3319−3322.

22. Nohra B, El Moll H, Albelo LMR, Mialane P, Marrot J, Mellot-Draznieks C, O'Keeffe M, Biboum RN, Lemaire J, Keita B. Polyoxometalate-based metal organic frameworks (Pomofs): structural trends, energetics, and high electrocatalytic efficiency for hydrogen evolution reaction. J. Am. Chem. Soc. 2011; 133: 13363−13374.

23. Zhang HY, Miao AJ, Jiang M. Fabrication, characterization and electrochemistry of organic-inorganic multilayer films containing polyoxometalate and polyviologen via Layer-by-Layer self- assembly. Mater. Chem. Phys. 2013; 141: 482−487.

24. Contant R. Relation entre les tungstophophates apparentés à l'anion $PW_{12}O_{40}^{3-}$. Synthèse et propriétés d'un nouveau polyoxotungstophosphate lacunaire $K_{10}P_2W_{20}O_{70} \cdot 24H_2O$, Can. J. Chem. 1987; *65*: 568-573.